Statistical Model Relating CA3 Burst Probability to Recovery From Burst-Induced Depression at Recurrent Collateral Synapses

KEVIN J. STALEY, JAIDEEP S. BAINS, AUDREY YEE, JENNIFER HELLIER, AND J. MARK LONGACHER
Departments of Pediatrics and Neurology, University of Colorado Health Sciences Center, Denver, Colorado 80262

Staley, Kevin J., Jaideep S. Bains, Audrey Yee, Jennifer Hellier, and J. Mark Longacher. Statistical model relating CA3 burst probability to recovery from burst-induced depression at recurrent collateral synapses. *J Neurophysiol* 86: 2736–2747, 2001. When neuronal excitability is increased in area CA3 of the hippocampus in vitro, the pyramidal cells generate periodic bursts of action potentials that are synchronized across the network. We have previously provided evidence that synaptic depression at the excitatory recurrent collateral synapses in the CA3 network terminates each population burst so that the next burst cannot begin until these synapses have recovered. These findings raise the possibility that burst timing can be described in terms of the probability of recovery of this population of synapses. Here we demonstrate that when neuronal excitability is changed in the CA3 network, the mean and variance of the interburst interval change in a manner that is consistent with a timing mechanism comprised of a pool of exponentially relaxing pacemakers. The relaxation time constant of these pacemakers is the same as the time constant describing the recovery from activity-dependent depression of recurrent collateral synapses. Recovery was estimated from the rate of spontaneous transmitter release versus time elapsed since the last CA3 burst. Pharmacological and long-term alterations of synaptic strength and network excitability affected CA3 burst timing as predicted by the cumulative binomial distribution if the burst pace-maker consists of a pool of recovering recurrent synapses. These findings indicate that the recovery of a pool of synapses from burst-induced depression is a sufficient explanation for burst timing in the in vitro CA3 neuronal network. These findings also demonstrate how information regarding the nature of a pacemaker can be derived from the temporal pattern of synchronous network activity. This information could also be extracted from less accessible networks such as those generating interictal epileptiform discharges in vivo.

INTRODUCTION

One goal of synaptic physiology is to understand the working of neural networks in terms of the properties of the synapses that connect the member neurons. However, the complexity of real neural networks (Churchland and Sejnowski 1992; Hampson et al. 1999; Marder 1998) makes it difficult to determine how various synaptic properties (Bains et al. 1999; King et al. 1999; Malenka and Nicoll 1999; Markram et al. 1998; Martin et al. 2000) affect network ouput. One approach to the complexity problem is to analyze synaptic influences on very simple modes of network behavior, such as the periodic, synchronous discharge of all neurons in the network. This "bursting" mode of activity is amenable to analysis because the outputs of all neurons in the network are so similar that to a first approximation they can be considered identical (Traub and Miles 1991). Further, the network activity can be simplified to two states: all neurons firing at high frequencies during the burst versus no or low-frequency firing between bursts (Cohen and Miles 2000).

The analysis of network bursts is further simplified because this mode of network operation does not depend on intact inhibitory conductances. Blockade of postsynaptic inhibition is one of the most robust ways to initiate burst activity in the CA3 network of the adult hippocampus (Traub and Miles 1991), and spontaneous bursts occur in CA3 during the developmental period during which the postsynaptic actions of GABA are excitatory (Leinekugel et al. 1997). In bursting networks studied to date, bursts appear to be terminated by activity-dependent depression at recurrent excitatory synapses (reviewed in Feller 1999; O'Donovan and Rinzel 1997) rather than postsynaptic feedback inhibition or calcium-activated potassium conductances (Robinson et al. 1993; Staley et al. 1998). Although the dissipation of inhibitory conductances can modulate the interburst interval, the period between discharges is primarily determined by the time required for the synapses to recover from depression (as proposed by O'Donovan and Rinzel 1997; Staley et al. 1998; modeled in Tabak et al. 2000; Tsodyks et al. 2000). Thus burst timing should reflect synaptic recovery in the network.

In this paper, we consider whether the recovery of a network of recurrent collateral synapses from burst-induced depression (Selig et al. 1999) could be a sufficient explanation for the timing of synchronous CA3 bursts. Periodic CA3 network bursts are readily elicited in the CA3 hippocampal network when neuronal excitability is increased (Johnston and Brown 1986; Traub and Wong 1982) due to the degree of positive feedback mediated by recurrent collateral glutamatergic synapses (King et al. 1999; Miles and Wong 1986; Traub and Miles 1991). The next CA3 burst begins when synapses recover sufficiently to generate spontaneous excitatory postsynaptic potentials (EPSPs) at a rate that triggers action potentials in some neurons (Chamberlin et al. 1990; Traub and Dingledine 1990). With each CA3 cell that reaches action potential threshold, the probability of recruiting subsequent CA3 cells increases due to additional action potential-dependent glutamate release. It follows that the probability of recruiting addi-

tional pyramidal cells must be at a minimum when the number of pyramidal cells firing synchronous action potentials is at a minimum; thus the time dependence of this probability should determine the timing of the next burst.

The probability of initiating and propagating the first synchronous action potentials should be highest at strong synapses, synapses whose postsynaptic neurons are close to action potential threshold, and synapses with high release probabilities (Bains et al. 1999; Dobrunz and Stevens 1997; Markram et al. 1998; Martin et al. 2000). If there are N such synapses, then the "depression recovery" hypothesis predicts that a burst will be initiated only when a sufficient number of these N synapses have recovered from the depression induced by the last burst. If K represents this sufficient number of synapses, then the probability of a network discharge at any point in time should be directly linked to the probability that K of N synapses have recovered from synaptic depression. Because the time course of synaptic recovery can be measured (Dittman et al. 2000; Markram et al. 1998; Stevens and Wesseling 1998), comparison of the time course of synaptic recovery to the mean and variance of the burst interval permits estimations of both N and K.

In this paper, we derive expressions relating N and K to burst timing. It was not possible to test these expressions directly by independent measurements of N and K. Instead, we tested the utility of these expressions by pharmacologically manipulating the strength of recurrent synapses, measuring the consequent changes in CA3 burst timing, fitting the interburst time interval distributions to the expressions for N and K and determining whether the changes in N and K predicted by the expressions are consistent with the pharmacological effects on synaptic function.

METHODS

Recordings

Hippocampal slices were prepared from adult rats as described previously (Staley et al. 1998). Recordings were performed in artificial cerebrospinal fluid (ACSF) at 35°C. ACSF was saturated with 95% O_2-5% CO_2 and included (in mM) 126 NaCl, 2.5 KCl, 26 NaHCO$_3$, 2 CaCl$_2$, 2 MgCl$_2$, 1.25 NaH$_2$PO$_4$, and 10 glucose. Whole cell pipette solutions contained (in mM) 123 cesium methylsulfonate, 2 MgCl$_2$, 8 NaCl, 1 potassium ethylene glycol-bis(b-aminoethyl ether) N, N,N',N'-tetraacteic acid (EGTA), 4 potassium ATP, 0.3 sodium GTP, and 1 N-(2,6-dimethylphenylcarbamoylmethyl) triethylammonium bromide (QX314) (for current-clamp experiments, Cs was replaced by K and QX314 was omitted). Whole cell solutions were buffered with 16 mM KHCO$_3$ and saturated with 95% O_2-5% CO_2. Extracellular recordings were performed using ACSF-filled whole cell pipettes placed in stratum pyramidale. Bursting in CA3 was induced by either increasing the K_o^+ to between 4.5 and 8.5 mM as noted in the text, or by one-time tetanic stimulation (100 Hz for 1 s) of the recurrent collateral system using a bipolar electrode placed in s. pyramidale (Staley et al. 1998). When bursts were induced by tetanic stimulation, final ACSF ionic concentrations were as described by Stasheff et al. (1989): (in mM) 1.3 Ca^{2+}, 0.9 Mg^{2+}, and 3.3 K^+. Long-term depression (LTD) of the recurrent synapses was induced by temporary partial block of the N-methyl-D-aspartate (NMDA) receptor during spontaneous network discharges using 40–100 μM DL-amino-5-phosphonovaleric acid (APV) (Bains et al. 1999). Evoked network discharges (Fig. 7, A and B) were triggered after every third spontaneous discharge by electrical stimulation in the pyramidal cell layer at an intensity that was sufficient to trigger a population spike prior to initiation of periodic discharges. Excitatory postsynaptic currents (EPSCs) were identified using a rectangular window (amplitude × duration), with amplitude set by eye to exclude baseline noise. Recordings were performed with an Axoclamp 2B amplifier (Axon Instruments, Foster City, CA) and digitized at 2-kHz using a PCI-DAS 1602/16 (Computer Boards, Middleboro, MA) and software written in visual basic 6.0. Drugs were obtained from Sigma (St. Louis, MO) and applied by bath.

Some of the experimental data in Figs. 4, 9, 10, and 11 have been previously published in aggregate form (Bains et al. 1999; Staley et al. 1998).

Data analysis

The cumulative probability of recovery from short-term depression at an individual synapse (p_1) has been derived in a number of preparations by fitting the response to evoked transmitter release to an exponential function (Dittman et al. 2000; Markram et al. 1998; Stevens and Wesseling 1998)

$$p_1 = 1 - e^{(-t/\tau)} \tag{1}$$

where τ is the time constant describing the recovery rate, and t is the time since the onset of depression. The same expression has also been derived by considering that the rate of recovery is proportional to the remaining number of empty release sites (Staley et al. 1998). Because the rate of recovery at each synapse may not be identical (Stevens and Wesseling 1998), in this study we estimated a population-average recovery rate from the rate of spontaneous EPSCs. Then *Eq. 1* can be considered to be the probability that a synapse has recovered sufficiently, if the average recovery rate is $1/\tau$ and synaptic recovery proceeds as a Poisson process (Bethea et al. 1995: the cumulative Poisson probability is also described by *Eq. 1*). For Poisson recovery, the probability of recovery is constant during a given interval of time so that as more time intervals elapse, the probability that a synapse has recovered increases with time constant τ.

The number of synapses that are capable of participating in burst initiation is denoted by N, and the number that must recover to initiate a burst is denoted by K. We assumed that all N synapses are uniformly depressed at the end of each burst, which seems reasonable given the high probability of transmitter release during action potential bursts (Selig et al. 1999). This uniform postburst depression implies that the current interburst interval is independent of prior intervals. If the N synapses recover from depression as described by *Eq. 1,* then we can greatly simplify the calculation of the probability of recovery of K of N synapses during the interburst interval by using the binomial distribution to estimate the probability that K synapses from a candidate pool of size N have recovered

$$P(N, K, p_1) = \left(\frac{N!}{K! \times (N - K)!} \right)(p_1)^K (1 - p_1)^{(N-K)} \tag{2}$$

The binomial distribution applies to binary (true/false) variables; we are considering synapses to be in two states, either recovered sufficiently to be capable of releasing transmitter during burst initiation, or not (Debanne et al. 1996).

We are interested in the probability that K *or more* synapses have recovered. The cumulative binomial probability distribution gives the probability that less than K synapses have recovered. The survival function, which is equal to one minus the cumulative binomial distribution (Hastings and Peacock 1975), therefore gives the probability that K or more of the N synapses have recovered. Thus the cumulative probability of a burst in the interval $(0, t)$ is given by

$$P_{\text{discharge}} = P(N, \geq K, p_1) = 1 - \sum_{X=1}^{X=K-1} P(N, X, p_1) \tag{3}$$

This is the probability that K or more of N synapses have recovered. The value of p_1 increases with time (*Eq. 1*), so the probability that K of N synapses have recovered also changes with time (Fig. 1).

How unique are the solutions provided by particular values of K and N? At any one point in time, for example 2 s after the last burst, many different values of N and K might provide a reasonable burst probability. However, to fit the experimental data, *Eq. 3* must be fit to the burst probability using the same values of N and K at *every* time interval using the corresponding value of p_1 calculated from *Eq. 1*. This severely constrains the acceptable values of N and K because the rate at which *Eq. 3* changes with time (which corresponds to the variance of the burst interval) depends on the difference between K and N (Fig. 2*B*), while the point at which the probability becomes significant (which corresponds to the mean burst interval) depends on the ratio of K to N (Fig. 2*A*).

Equation 3 was fit to the cumulative probability plots of the interburst intervals using 50–100 time increments and least-squares estimates of goodness of fit to the cumulative probability of the burst interval. The incomplete beta function was used to calculate the cumulative binomial distribution (Press et al. 1997). *Equation 1* was fit to EPSC rates at postburst intervals before the probability of a subsequent discharge became significant (Fig. 6*B*) and the EPSC rate became unstable (Fig. 6, *B* and *C*), using the least-squares method. *Equation 1* was also used to fit the length of bursts evoked at variable intervals after a spontaneous burst to assay the degree of synaptic recovery (Staley et al. 1998), a method analogous to compound EPSC amplitude measurements in paired pulse paradigms (Markram et al. 1998). This fit was only relevant
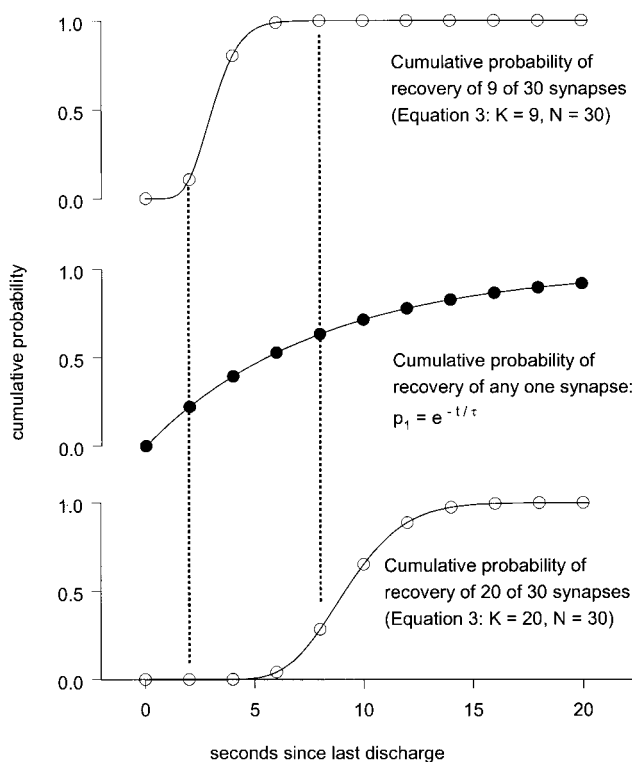

FIG. 1. Relationship between probability of recovery of 1 synapse vs. the probability of recovery of a pool of synapses. *Middle*: the probability of recovery of one synapse based on *Eq. 1*. *Top* and *bottom*: the probability of recovery of a fraction of a pool of 30 such synapses. For the *top panel,* the cumulative probability of recovery of 9 of 30 synapses is illustrated using *Eq. 3*. The *bottom panel* illustrates the cumulative probability that 20 of 30 synapses have recovered. - - -, for a given probility of recovery at an individual synapse, the probability that a fraction of a pool of such synapses has recovered is strongly dependent on the size of the fraction.
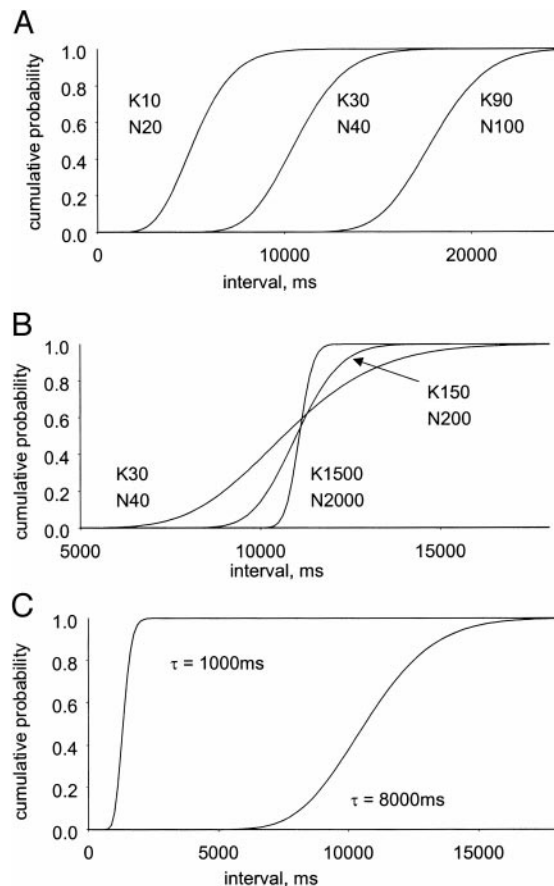

FIG. 2. Behavior of the survival function. A time constant of 8 s is used in these examples. *A*: the difference between N and K determines the slope of the survival function. When $(N - K)$ is constant, variations of N and K shift the curve to the left or right without changing the slope. *B*: the ratio of K to N determines the position of the curve on the ordinate. When (N/K) is constant, varying N and K changes the slope but has minor effects on the position of the rising portion curve. *C*: changing τ affects both the position of the survival function on the ordinate and the shape of the survival function. τ was fixed at 8 s in all fits of experimental data.

when the stimulus was sufficiently large to preclude burst initiation failure (Fig. 7*B*).

RESULTS

Probability distribution of interburst intervals

We induced stable periodic population bursts in hippocampal area CA3 in vitro by either long-term potentiation (LTP) of recurrent collateral synapses (Bains et al. 1999) or by increasing the concentration of extracellular potassium (K_o^+) above 4.5 mM (Fig. 3, *A* and *B*; $n = 145$ slices). The intervals between bursts were normally distributed for all conditions (Fig. 3, *C* and *D*) (Robinson et al. 1993). Increasing network excitability by increasing K_o^+ from 5.5 to 10.5 mM altered the frequency of bursts by over 6 octaves, from <0.05 Hz in 5.5 mM K_o^+ to 1 Hz in 10.5 mM K_o^+ (Fig. 4, *A* and *B*). For each change in K_o^+, the corresponding burst intervals were normally distributed about the mean (Fig. 4*B*) and the variance of the intervals increased with the third power of the mean (Fig. 4*C*).

The nonlinear relationship between the variance and the mean of the discharge interval (Fig. 4*C*) is not easy to reconcile with a single pacemaking mechanism whose probability
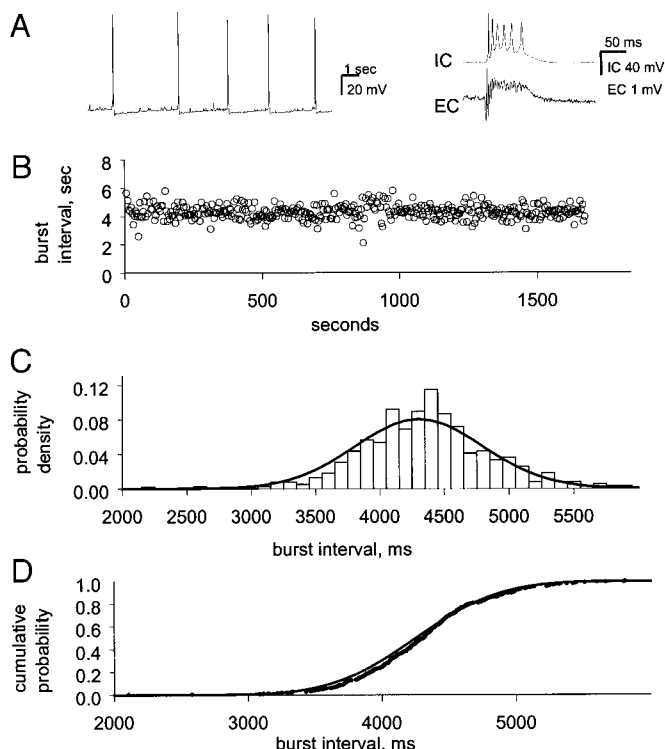
FIG. 3. The intervals between CA3 population bursts are normally distributed. *A, left*: a whole cell recording from a pyramidal cell demonstrating the temporal pattern of spontaneous CA3 discharges in 8.5 mM K_o^+. *Right*: paired recordings from a pyramidal cell (IC) and the pyramidal cell layer (EC) demonstrating that the CA3 network discharges are a synchronous, all-or-none process. *B*: plot of the intervals between spontaneous CA3 population bursts demonstrates a stable mean burst interval over 30 min. *C*: intervals in *B* are normally distributed: a histogram of intervals binned at 100-ms intervals is well fit by the normal distribution (—). *D*: unbinned cumulative probability plot of the data shown in *C* and the cumulative normal distribution (—).

changes with network excitability. Neither a Poisson nor a binomial distribution can describe the observed relationship between the mean and the variance of the burst intervals (Bethea et al. 1995; cf. Reid and Clements 1999). Rather, this relationship supports the idea that a process such as recovery from synaptic depression (*Eq. 1*) of a population of synapses is the primary determinant of the burst interval: because the probability of recovery of a single synapse (*Eq. 1*) increases rapidly at short time intervals and more slowly at longer time intervals (Fig. 5*A*), the survival function (*Eq. 3*) has a very tight time distribution for short time intervals and a much broader distribution at longer intervals for any given *N* and *K* (Fig. 5, *B* and *C*). In fact, the probability of recovery of *K* synapses from among a candidate pool of size *N* has the same relationship between the variance and the mean as the experimentally observed probability of a burst (Fig. 4*B* vs. 5*C*; the data in Fig. 4*B* are fit by *Eq. 3* in Fig. 11*A*).

Estimating the time constant for recovery from synaptic depression

To determine the time constant for recovery from depression at individual synapses (*Eq. 1*), we measured the rate of spontaneous transmitter release (Liu and Tsien 1995; Otis et al. 1996; Stevens and Wesseling 1998). The frequency of spontaneous EPSCs was measured as a function of time after a burst

(Fig. 6, *A* and *B*). Although the postburst spontaneous EPSC rate should reflect a variety of processes such as diminishing facilitation (Dittman et al. 2000), the monoexponential increase suggests that the EPSC rate is dominated by recovery from depression. At short postdischarge intervals, the frequency of EPSCs increased with a time constant of 8 ± 2.3 (SD) s (*n* = 8 cells; Fig. 6*B*). The measured EPSC recovery rate is similar to the rate of recovery in single-synapse studies of these neurons (Stevens and Wesseling 1998) and is of the same order of magnitude as the intervals between spontaneous bursts (e.g., Fig. 4*B*). The EPSC rates at longer intervals from the last burst discharge fluctuated widely, consistent with action-potential-dependent transmitter release (Fig. 6, *B* and *C*) as a consequence of the positive feedback mediated by the recurrent collateral synapses (Traub and Dingledine 1990; Traub and Miles 1991). There was no correlation between the EPSC recovery rate measured from a single cell recording and the interburst interval in the slice from which the cell was recorded, consistent with the idea that synaptic recovery does not vary from slice to slice so that the variation in the measured EPSC recovery rate represented sampling error (1 pyramidal cell of the thousands in the slice) rather than a systematic difference in synaptic recovery rates between slices. We used a fixed recovery time constant of 8 s to fit the data in all subsequent experiments.

Shorter time constant obtained by measuring evoked release

The 8-s time constant for synaptic recovery assayed by EPSC frequency is longer than the time constant of recovery assayed using osmotically and electrically evoked transmitter release (Staley et al. 1998). When bursts were evoked at various time intervals following a spontaneous burst, synaptic recovery as assayed by the evoked burst length was too rapid to explain the interval between discharges: evoked burst length was already maximal when the probability of a spontaneous burst was still negligible (Fig. 7*A*). It has recently been demonstrated that during recovery from synaptic depression, large stimuli can evoke transmitter release when small stimuli cannot (Stevens and Wesseling 1998; Wu et al. 1999; modeled in Mateev and Wang 2000). Thus one explanation for the difference in spontaneous versus evoked recovery may be the size of the depolarization and the number of cells that are synchronously depolarized by the electrical stimulus versus a spontaneous EPSP. If this was true, then it would be expected that smaller external stimuli should be less effective at triggering bursts at short postburst time intervals. This effect is illustrated in Fig. 7*B*: stimuli of two different amplitudes were delivered through the same electrode using the same protocol as for the experiment illustrated in Fig. 7*A*. The large stimulus was sufficient to evoke the maximum-amplitude population spike before the induction of bursting. The smaller stimulus was sufficient to evoke a just-detectable population spike. The duration of the burst evoked by either of these two stimuli, each delivered at random intervals after a spontaneous burst, is plotted in Fig. 7*B*. The smaller stimuli resulted in more failures of burst initiation when delivered at short intervals following a spontaneous burst. The resulting sigmoidal, rather than exponential, relationship between evoked burst length and the interval since the last burst resembled the cumulative probability distribution of spontaneous burst initiation (Fig. 7, *A* and *B*; see

also Figs. 3*D* and 4*B*), as well as the probability of evoking a burst when a single neuron is stimulated (Miles and Wong 1983). Thus the rate of recovery from depression varies as a function of the stimulus used to measure it as demonstrated in other systems (Stevens and Wesseling 1998; Wu et al. 1999; modeled in Mateev and Wang 2000). Because spontaneous bursts are initiated by EPSPs (Chamberlin et al. 1990; Traub and Dingledine 1990), we used the 8-s time constant established by the experiments shown in Fig. 6 for our calculations.

Fitting interburst interval probability distributions to the survival function

Once the time course of synaptic recovery is known (Fig. 6*B* and *Eq. 1*), it should be possible to predict the probability of a burst from the probability of recovery of the appropriate number of synapses (i.e., the probability that K synapses from a pool of N candidate synapses have recovered, *Eq. 3*). The best test of this idea would be to experimentally determine the value of K and N and then use these values to predict the burst probability. In the absence of a means to determine K or N directly, we tested the validity of *Eq. 3* by fitting it to the burst probability, thereby deriving the values of K and N. Although there is no direct method to test whether these fitted values correspond to the actual numbers of synapses involved in burst initiation, we can test two predictions that follow from the idea
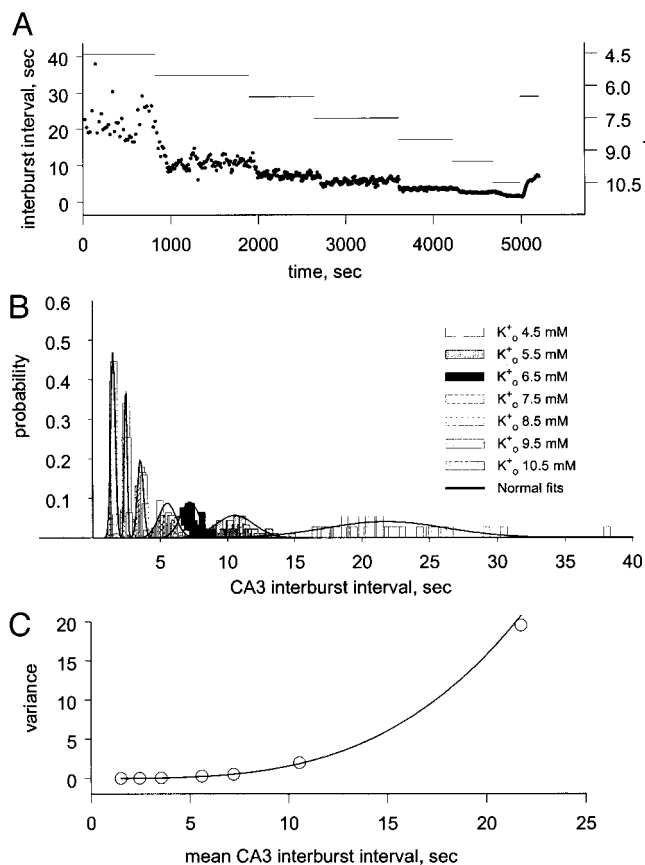

FIG. 4. The mean vs. variance of the interburst interval. *A*: interval between CA3 network discharges vs. K_o^+ (—). The level of neuronal excitability alters the interval. *B*: intervals from the experiment shown in *B* are normally distributed for each level of K_o^+. —, fit normal distributions. *C*: variance of the discharge intervals shown in *B* and *C* increase with the 3rd power of the mean (—: variance = $0.007 \times$ mean$^{3.3}$).
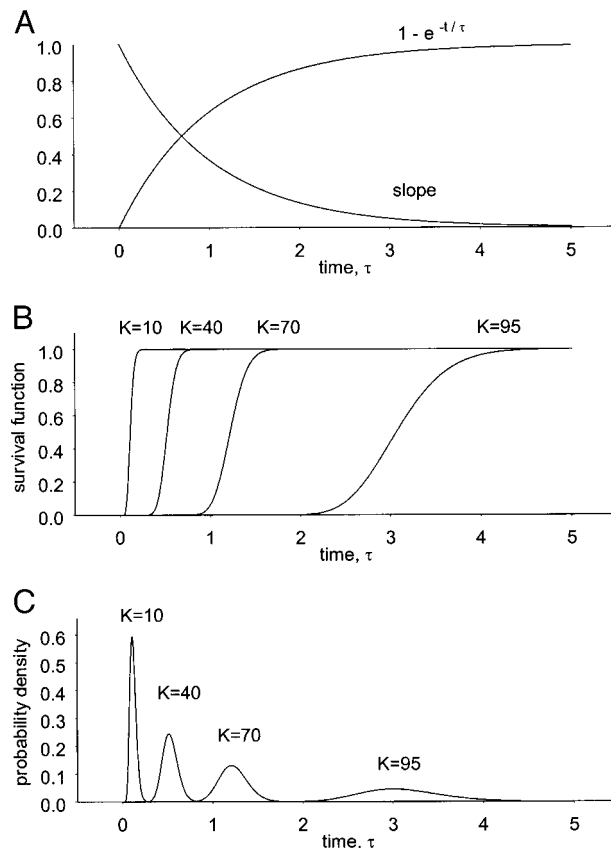

FIG. 5. The survival function has the same relationship between the mean and the variance as the CA3 burst interval distribution. *A*: plot of *Eq. 1*, the cumulative probability of recovery from depression at a single synapse. The rate of recovery (time derivative of *Eq. 1*) is maximal for small time intervals. Time is plotted as multiples of the time constant τ. *B*: plot of survival function (= 1 − cumulative probability distribution; *Eq. 3*) for a population of $n = 100$ and the values of K noted in the figure. *C*: the mean and variance of the probability density of the survival function (derived by differentiation from the cumulative probability distributions shown in *B*) change in a manner similar to the network discharge probability density (Fig. 4*B*).

that CA3 bursts occur when a sufficient number of the pool of initiating synapses have recovered from depression. First, the size of the initiating pool should be directly reflected in the probability of a CA3 discharge. Second, manipulations of either neuronal excitability or synaptic strength should change N, the number of synapses at which transmitter release significantly increases the probability of successful initiation of a burst. Manipulations of either neuronal excitability or synaptic strength should also produce a corresponding change in K, the number of synapses whose recovery is necessary to initiate a burst.

To test these predictions, synaptic strength was decreased up to 50% using either low concentrations of the competitive non-NMDA antagonist 6,7-dinitroquinoxaline-2,3(1H,4H)-dione (DNQX) (Andreason et al. 1989; Chamberlin et al. 1990) ($n = 7$; Fig. 8, *A* and *B*), decreasing release probability with baclofen (Scanziani et al. 1992; Swartzwelder et al. 1987) ($n = 8$; Fig. 9, *A* and *B*), or by long-term depression (LTD) of the recurrent synapses (Bains et al. 1999; Cummings et al. 1996; Lisman et al. 1989) ($n = 4$; Fig. 10, *A* and *B*). All three methods of decreasing the synaptic strength increased the mean and variance of the burst interval. These changes were well-fit

by *Eq. 3* (— in Figs. 8, *A* and *B*; 9, *A* and *B*; and 10, *A* and *B*). The fit values of *N* and *K* are shown in Figs. 8*C*, 9*C*, and 10*C*.

Baclofen and DNQX both decreased the average synaptic strength and thus decreased *N*, the number of synapses capable of participating in burst initiation. These agents had different effects on *K*, however. One way to interpret the differential effect on *K* is in terms of the effects of baclofen and DNQX on inter-burst depression. Depression should be similar at the end of a burst for both agents due to the degree of facilitation of release during a burst (Selig et al. 1999). However, between bursts baclofen decreases the probability of release (Debanne et al. 1996) and thus the degree of ongoing depression from spontaneous EPSCs; thus the network may be more able to respond to an initiating EPSP, which would be reflected in decreased values of *K*.

Neuronal excitability was altered by changing K_o^+ (Fig. 11, *A* and *B*; *n* = 7). Decreasing the network excitability produced a corresponding decrease in the size of the pool of synapses that were capable of initiating a burst and increased the fraction of the pool that needed to recover (Fig. 11*B*). When network excitability is increased, bursts are more likely to be initiated at shorter interburst intervals (Fig. 11, *A* and *B*) when the degree of synaptic recovery is less complete. This decreased recovery should be reflected in the burst duration, as is the case for evoked bursts (Fig. 7). Figure 11*C* plots the duration of spontaneous bursts versus the interval since the last burst for the experiment in which K_o^+ was varied. The burst duration in-

FIG. 7. Synaptic recovery assayed by evoked network discharges. *A*: comparison of the recovery rate assayed by evoked CA3 burst length vs. the cumulative probability of a spontaneous burst. The degree of synaptic recovery was assayed by the length of a burst evoked at various time intervals after a spontaneous burst (●), and fit to *Eq. 1* (—; τ = 1.2 s). The synaptic recovery assayed in this way was essentially complete when the probability of a spontaneous CA3 burst (○) was still minimal. *B*: the time course of synaptic recovery approaches the cumulative probability of spontaneous burst intervals as the stimulus strength is decreased. Synaptic recovery was assayed by the duration of evoked bursts as in *A*. ●, duration of bursts evoked at random intervals following the last burst by a large stimulus. Line fit to large stimulus data using *Eq. 1*, τ = 500 ms. ◑, duration of bursts evoked at random intervals following the last burst by a smaller stimulus. ⋯, SEs. The SE for the smaller stimulus is maximal on the rising portion of the curve due to the mixture of burst initiation failures and successes. Small stimulus burst lengths were fit using a polynomial, because neither *Eq. 1* nor *3* was appropriate to fit evoked burst lengths with failures. ○, cumulative probability of intervals between spontaneous bursts. —, *Eq. 3* fit to the interval data with *K* = 10, *n* = 11. (The stimulation protocol cannot be accurately extended to intervals that overlap with the spontaneous burst interval because under such conditions a second spontaneous burst may occur in the interval between the initial burst and the evoked burst, resulting in additional synaptic depression.)
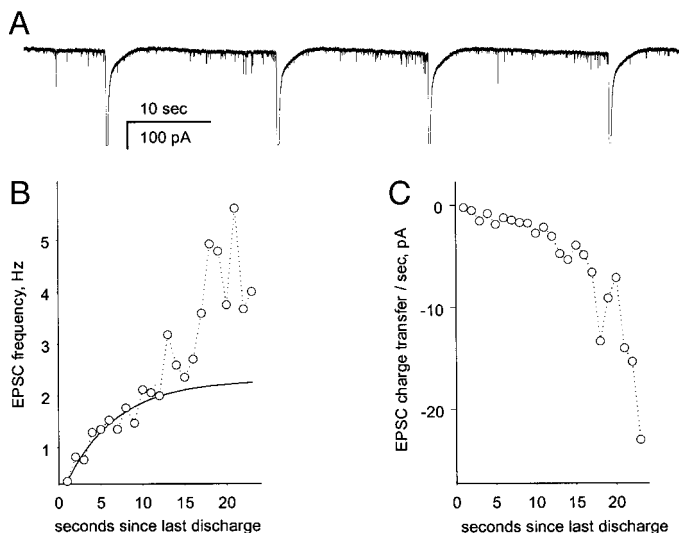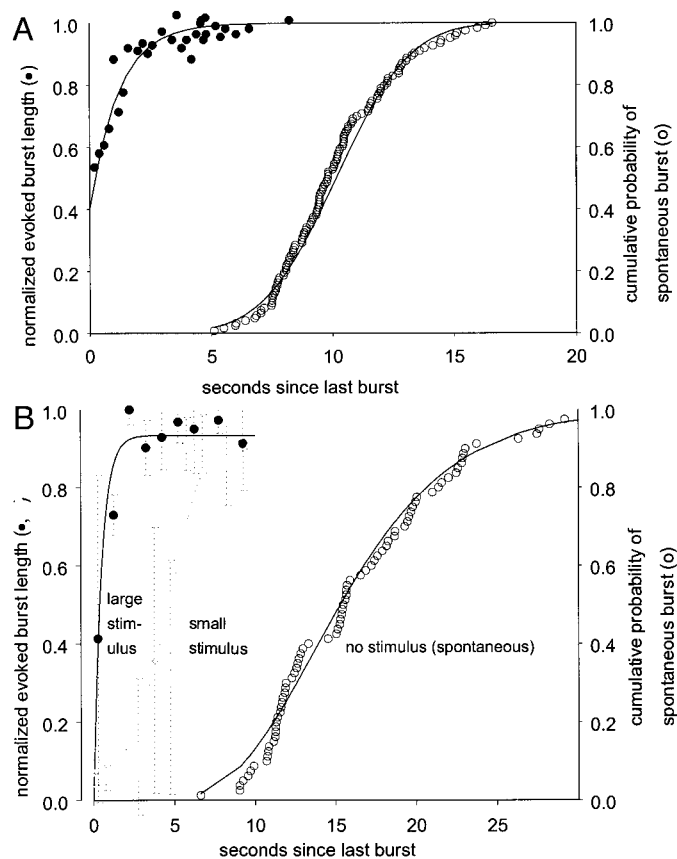

FIG. 6. Synaptic recovery assayed by spontaneous synaptic activity. *A*: an example of excitatory postsynaptic currents (EPSCs) recorded between network discharges at a holding potential of −60 mV after induction of discharges by a single tetanization. Clusters of EPSCs occur near the start of a network discharge (Traub and Dingledine 1990). Afterhyperpolarizations were antagonized by 20 μM norepinephrine in these experiments (Staley et al. 1998), and GABA_A receptors were blocked with 100 μM picrotoxin. *B*: the frequency of EPSCs is plotted vs. the time elapsed since the end of the last discharge. —, a fit of *Eq. 1* to the initial 12 s of data with τ = 6 s. The EPSC frequency becomes unpredictable at intervals closer to the average discharge interval, which was 20 s in this experiment. EPSCs recorded at a potential of −60 mV after induction of CA3 discharges using a tetanic stimulation. *C*: the charge transfer (area) of the EPSCs plotted in *B* shows a greater increase with time than the EPSC frequency, consistent with action potential-dependent amplification [the increase in EPSC amplitude is not due to postburst changes in dendritic space clamp (Staley and Mody 1992) because input resistance returned to within 95% of preburst baseline within 3 s after a burst, *n* = 3 cells (Robinson and Deadwyler 1981; Staley et al. 1998)].

creases with a time constant of 6 s, close to the rate of synaptic recovery measured from the EPSC rates (Fig. 6*B*). There is no relationship between spontaneous burst length and interburst interval for any given K_o^+ (Fig. 11*C, insets*). This indicates that recovery from depression is the timing mechanism for burst intervals: if burst duration were determined by the degree of synaptic recovery, but an independent timing mechanism (such as dissipation of inhibition) determined burst intervals, then for any given experimental condition the burst duration versus interval plots (Fig. 11*C, insets*) would show the same relationship between burst interval and duration as do the independently timed evoked bursts in Fig. 7, *A* and *B*.

DISCUSSION

We conclude that a under a variety of experimental conditions, the temporal pattern of CA3 network output can be accurately fit using a pool of exponentially relaxing pacemakers. The time constant describing the relaxation of these pacemakers is the same as the time constant describing the recovery of recurrent collateral synapses from activity-induced depression. Long and short-term determinants of synaptic strength and the level of network excitability affect the distribution of CA3 interburst intervals as predicted if these manipulations affected the total number of synapses in the pacemaking pool (i.e., N, the synapses capable of participating in burst initiation), and the number of synapses in the pacemaking pool that must recover before another spontaneous burst is possible (K).

Physiological significance of the fit parameters

In the experiment illustrated in Fig. 7B, the calculated number of synapses capable of initiating a burst discharge is 11. If these 11 synapses could be selectively blocked, bursts might continue, but at a somewhat lower frequency. This is because N can only be determined for a specific experimental condition and does not reflect the number of intact recurrent collateral
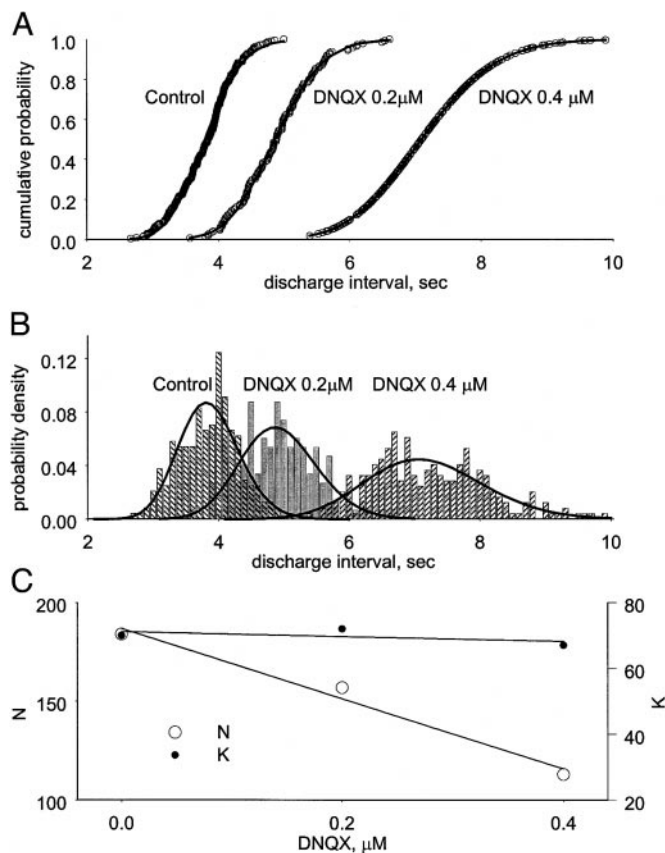

FIG. 8. The probability of network output is changed when synaptic strength is decreased by low concentrations of an AMPA antagonist. Synaptic strength was altered by decreasing the postsynaptic receptor availability with 6,7-dinitroquinoxaline-2,3(1H,4H)-dione (DNQX). A: the cumulative burst interval probability is plotted for control conditions (8.5 mM K_o^+), during bath application of 0.2 μM DNQX and during application of 0.4 μM DNQX. B: the corresponding probability densities for the data shown in A. — in A and B are best fits of Eq. 3 to the data. C: the fit values of K and N vs. the DNQX concentration.
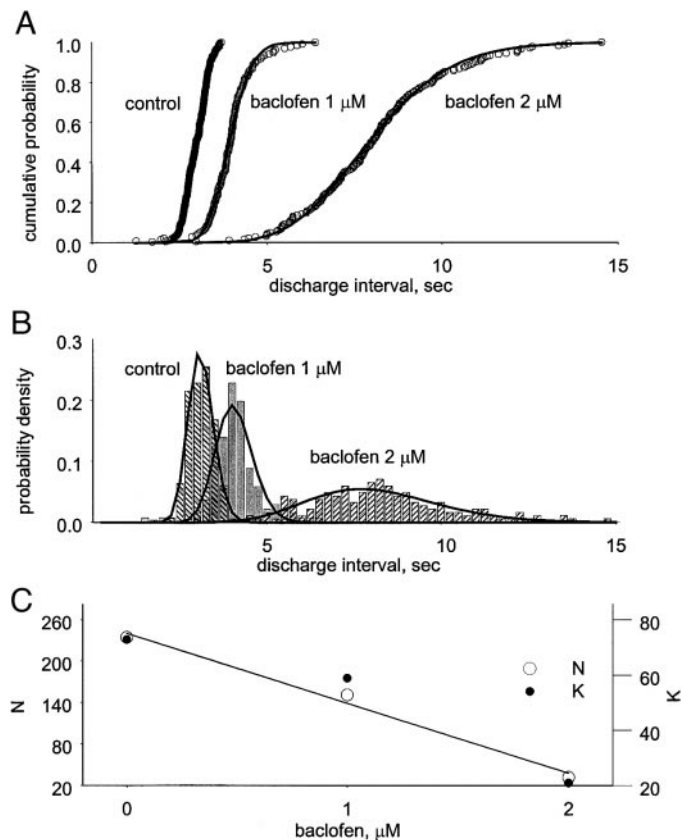

FIG. 9. The probability of network output is changed by decreasing the probability of transmitter release with baclofen. A: the cumulative burst interval probability is plotted for control conditions (8.5 mM K_o^+), during bath application of 1 μM baclofen and during application of 2 μM baclofen. B: the corresponding probability densities for the data shown in A. — in A and B are best fits of Eq. 3 to the data. C: the fit values of K and N vs. the baclofen concentration.

connections in the slice except perhaps as a limit at maximal excitability (Fig. 11, B and C). Further, N may not represent the very strongest synapses or those with the highest probability of release: ongoing transmitter release during the interburst interval (Fig. 6A) re-depresses the synapses that release transmitter too far in advance of burst initiation. These synapses could be stronger or have a higher probability of release than the N synapses that actually participate in burst initiation.

K, the number of synapses that need to recover to initiate a burst, also changes with experimental conditions. Immediately after a burst, synapses are depressed and excitability is correspondingly low, so K is large. For example in Fig. 7B, most smaller stimuli failed to initiate bursts for the first second after a spontaneous burst. This indicates that during the first second after a burst time interval, K was larger than the number of synapses activated by the smaller stimulus. As synapses recover and excitability increases, the number of synapses that are needed to initiate a burst decreases, so the smaller stimulus became sufficient to initiate a burst. It is important to note in terms of the assumptions underlying the derivation of Eq. 3 that this decrease in K is complete by the time a spontaneous burst is likely (in Fig. 7, the postburst time interval at which small stimuli trigger bursts as efficiently as large stimuli is shorter than the shortest spontaneous interburst interval). This result is not an artifact of the choice of stimulus sizes because

Miles and Wong obtained similar results with single-cell stimulation (Miles and Wong 1983).

The tendency of K to change in the same direction as N (Figs. 8–11 and 12A) may seem counterintuitive. As network excitability increases, more synapses are capable of initiating a burst, so N increases; it seems that with increasing excitability there should be a corresponding decrease in the number of synapses needed to initiate a burst (K). The fraction of synapses in the initiating pool that need to recover does indeed decrease with increasing excitability (Fig. 12B). However, the absolute number of synapses required increases due to the increase in the size of the initiating network of synapses.

There are many potential biological correlates of N and K. For instance, the decay of inhibitory conductances is a candidate determinant of burst probability (Traub and Miles 1991). Because blocking these conductances does not alter burst probability significantly, we favor the idea that synaptic depression terminates bursts and recovery from depression limits the probability of burst initiation (Staley et al. 1998). The large impact of small alterations of synaptic strength on the burst probability (Figs. 8–10) (Bains et al. 1999) supports the idea that recovery from synaptic depression is an important determinant of the probability of network discharge (modeled in Tabak et al. 2000; Tsodyks et al. 2000). For instance, if a pacemaker

FIG. 11. Effect of network excitability on burst probability. *A*: *Eq. 3* (—) fit to the network output intervals plotted in Fig. 4, *A* and *B*. *B*: the values of N and K for the fits shown in *A*. The pool size (N) varies from a few dozen to several thousand, and the number required to recover (K) varies from >90 to <20% of N. *C*: the rate of synaptic recovery can be estimated from the duration of the spontaneous bursts (plotted in *A*) vs. the interburst interval. *Insets*: there is no relationship between the interburst interval and the spontaneous burst length for any single level of excitability. The highest (10.5 mM K_o^+) and lowest (4.5 mM K_o^+) network excitabilities are shown.

current was the sole determinant of burst timing, altering synaptic strength should have a more significant effect on burst duration (as in Fig. 7) (see also Staley et al. 1998) rather than the interval between bursts (Fig. 11C, *insets*).

How EPSP amplitude, resting membrane potential (RMP), and action potential threshold influence N and K is unknown. Understanding the number of coincident EPSPs that are necessary to trigger an action potential would clarify burst initiation, but this will require a more detailed knowledge of dendritic EPSP algebra (Magee et al. 1998). Such information would help elucidate how postsynaptic inhibition by increasing the number of EPSPs required to initiate an action potential (Miles et al. 1996) modulates the probability of synchronous network activity.
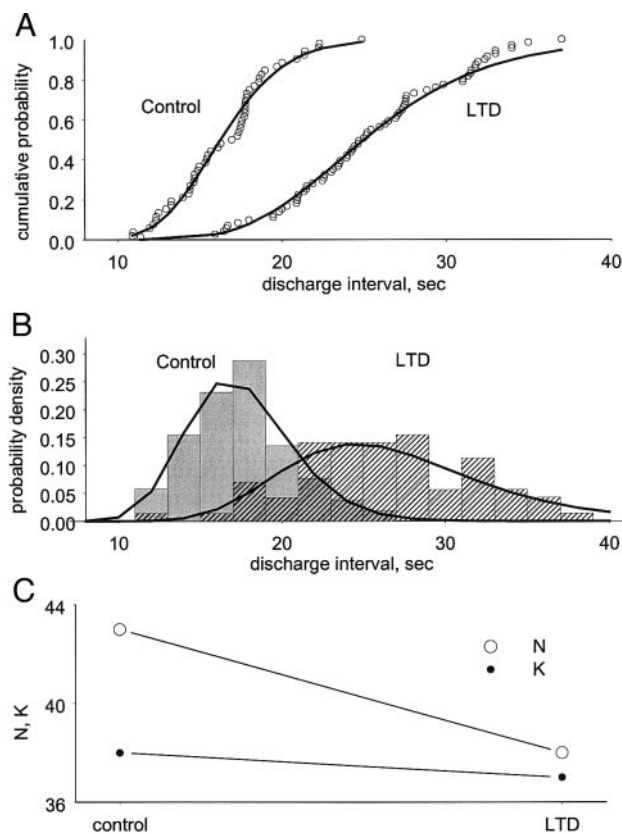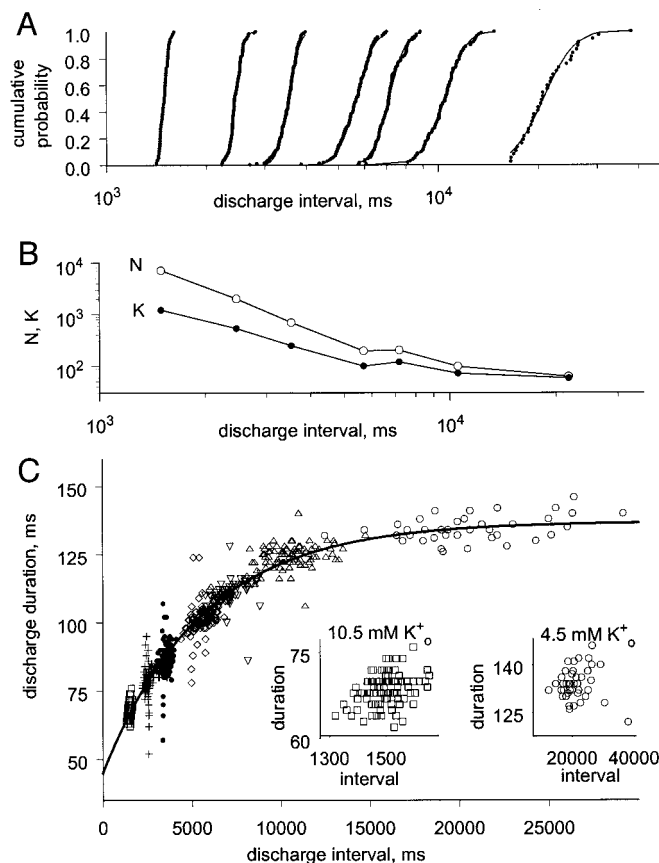

FIG. 10. The probability of network output is changed by long-term depression (LTD), the strength of the recurrent collateral synapses. LTD was induced by application of 40 μM of the competitive *N*-methyl-D-aspartate (NMDA) antagonist, D,L-APV during spontaneous CA3 bursting that had been induced by tetanization (Bains et al. 1999; Cummings et al. 1996; Lisman 1989). *A*: the cumulative burst interval probability is plotted before and after LTD. *B*: the corresponding probability densities for the data shown in *A*. — in *A* and *B* are best fits of *Eq. 3* to the data. *C*: the fit values of K and N before and after LTD.

Limitations

The binomial analysis is based on the related assumptions that the outcome of any one trial does not depend on the others, that the probability of success (p_1) is the same for all N trials and that all trials are identical. Trials here correspond to the burst probability for each time increment. Because the number of active neurons in one time interval affects the number of
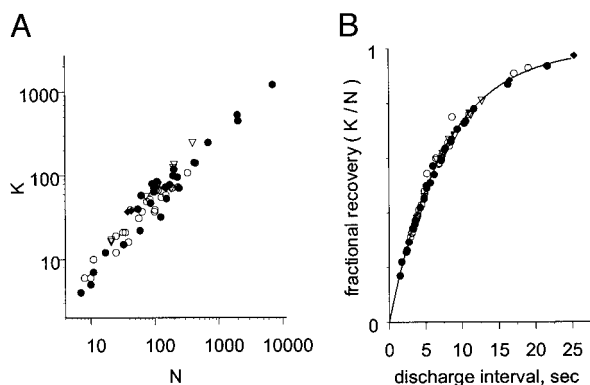
A

B

FIG. 12. Relationship between the size of the initiating pool of synapses (N), the number of synapses required to recover to initiate a network output (K), and the probability of network output. *A*: the range of values of N and K computed for the experiments shown in Figs. 8–11: DNQX ($\triangledown$), baclofen ($\bigcirc$), LTD ($\blacklozenge$), and K_o^+ ($\bullet$). The average ratio of K to N was 0.55 ± 0.19. *B*: the fraction of the pool required to recover to initiate a burst (K/N) increases as the probability of network output decreases (increased interval between network outputs, corresponding to decreased network excitability). Pooled data from the experiments shown in Figs. 8–11; symbols as in *A*. — fit by *Eq. 1* with $\tau = 8$ s.

active neurons in the next, trial-to-trial independence implies that in this model N does not represent the number of spontaneously active neurons (Butts et al. 1999). The assumption that p_1 is identical for all trials is strictly true only as a population average because the rate of recovery of individual synapses may vary (Stevens and Wesseling 1998). The assumption that all trials are identical implies that any combination of K or N synapses can initiate bursts. However, there may be circuits in which some synapses are more important than others, which would violate this assumption.

This analysis assumes that variation in burst timing is a consequence of variation in the recovery probability of K synapses; the variation in the time required for the recovered synapses to initiate a burst is neglected. If the time between recovery and burst initiation is substantial, it would lead to an inaccurate estimate of K (e.g., Fig. 2A). The frequency of EPSCs (Fig. 6) and action potentials (Cohen and Miles 2000) in the intervals between bursts suggests that adequate stimuli for burst initiation are continuously present. The similarity in the variance in CA3 burst initiation failures when a known population of synapses is activated (Miles and Wong 1983) (Fig. 7B) versus the variance of spontaneous intervals (e.g., Fig. 7, A and B) also suggests that synaptic recovery is the main source of variation, but this needs to be studied systematically. For instance, *Eq. 1* could be modified to a more general expression of the probability of achieving sufficient interburst synaptic strength, where synaptic strength is the product of the degree of depression, the baseline probability of release, and the postsynaptic effect. The last two terms can be combined as a term multiplying *Eq. 1*: $A_o \times (1 - e^{-t/\tau})$. Then if synapses are substantially weakened either pre- or postsynaptically, full recovery of p_1 would still leave the probability of achieving full synaptic strength at <1 (Fig. 1, *middle*) because A_o would be <1; under those conditions, much longer interburst intervals can be accommodated, but at the cost of another fitted variable. Verification would require dual recordings of synaptically connected pyramidal cells to ascertain A_o.

We have not considered variations in τ, the time constant for

recovery from synaptic depression at a single synapse, as an explanation for burst timing. Although τ clearly affects *Eqs. 1–3* (Fig. 2C), τ was fixed at 8 s for two reasons. First, we wished to limit the number of free variables in the fits. Second, the manipulations shown in Figs. 9–11 affect burst interval but do not affect τ (e.g., Fig. 6D of Staley et al. 1998). However, other experimental manipulations, such as alterations of calcium homeostasis in the synaptic terminal, might affect τ (Dittman et al. 2000; Stevens and Wesseling 1999).

The information provided by this model, the burst probability as a function of time, is much more limited than information provided by models that describe the activity of every cell in the network (Traub and Miles 1991) or the spatial distribution of network activity (Butts et al. 1999). The limited predictions of this model allow the number of free parameters to be limited to the experimentally determined synaptic recovery rate and the fit parameters N and K. More detailed network models should provide additional insights into relationship of network behavior and the degree of synaptic depression and recovery as well as the most accurate physiological correlates of these parameters.

Definitive proof of the depression recovery model of burst timing requires measurement and manipulation of N and K to test whether the manipulations affect burst timing as *Eq. 3* predicts. This could be approached qualitatively by sectioning the CA3 network and comparing burst interval distribution to the size of the remaining network (Miles et al. 1984). This issue might be studied quantitatively in autaptic cell cultures, where high degrees of synaptic positive feedback produce discharge patterns similar to CA3 bursts (Segal and Furshpan 1990). In the autaptic preparation, the number and activity of feedback synapses can be quantified (Prange and Murphy 1999) and manipulated (Liu et al. 2000).

Comparison to "recovering pacemaker current" model

Pacemaker currents such as I_H have been proposed to underlie several oscillatory network behaviors (McCormick and Pape 1990). This model of burst timing could also be described by *Eq. 3*: if the pacemaker conductance was inactivated by the membrane depolarization that occurred during the CA3 burst and if the conductance recovered from inactivation with first-order kinetics during the interburst interval, then N could represent the pool of pacemaking neurons, and K could represent the subset that needed to have their pacemaking conductances reach a particular threshold of de-inactivation to trigger a burst discharge.

A disadvantage of the "recovery to noisy threshold" model when applied to pacemaking neurons is that the recovery of the whole cell pacemaker conductance should not be probabilistic because whole cell recovery is the average of the recovery of a very large number of stochastically recovering channel proteins. Thus the trick of equating a recovery rate to a probability (*Eq. 1*) is not as easy to support for neurons as it is for individual synapses, which are known to behave in a stochastic manner (Fatt and Katz 1952). A physiological disadvantage of I_H as a pacemaking conductance is that I_H has a net inhibitory effect in hippocampal pyramidal cells (Magee 1998) and thus is not well suited to initiate CA3 bursts; further, CA3 bursts
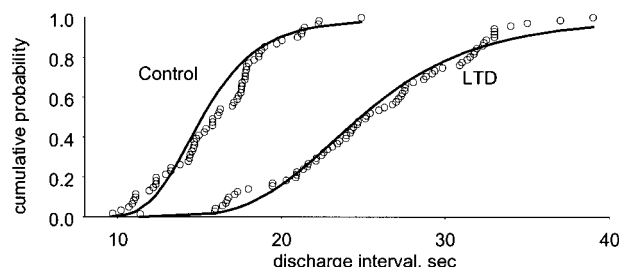
FIG. 13. The interburst interval distribution can be fit with a model employing relaxation of a first-order process (*Eq. 1*) to a noisy threshold. If the threshold's probability is normally distributed, the interburst intervals can be described by *Eq. 3* with the cumulative normal distribution used instead of the cumulative binomial distribution. The LTD data shown in Fig. 9 are fitted here by least squares with a relaxation time constant of 8 s. In control conditions, the threshold = 0.85 ± 0.052, and after LTD, the threshold was 0.955 ± 0.03 (means ± standard deviaton).

proceed normally after I_H is blocked (Xiong and Stringer 1999).

Instead of a pacemaking conductance, the rate-limiting recovery process that sets the CA3 interburst interval might be the de-inactivation of a voltage-dependent depolarizing membrane conductance to a particular threshold value. Examples might be dendritic conductances that amplify EPSPs, such as the dendritic sodium conductance or low-threshold calcium conductance (Magee et al. 1998). If the threshold to which the conductance needed to recover varied from burst to burst, then the binomial distribution used in *Eqs. 2* and *3* might be replaced by a normal distribution that describes the average value and standard deviation of this probabilistic threshold. As shown in Fig. 13, the recovery of a membrane conductance to a noisy threshold also fits the data.

A physiological disadvantage of the recovery to noisy threshold model is that there are no known pacemaking or voltage-dependent depolarizing conductances that have an inactivation recovery time constant in the range (~8 s at 35°C) that fits the interburst interval data (Magee 1998; Mickus et al. 1999), although it is conceivable that second-messenger regulation of a pacemaker conductance might have the appropriate kinetics. Further, manipulation of the known candidate conductances does not produce the expected effects on burst intervals. For example, blocking I_A negates most of the effects of dendritic sodium current inactivation (Colbert et al. 1997), but the intervals between CA3 bursts induced by the I_A antagonist 4AP are similar to those induced by other means (Traub and Miles 1991). A conceptual disadvantage of the recovery to noisy threshold model is that the threshold to which the conductance must recover to trigger a burst is described by a mean and SD that have no easily testable physiological interpretation (Fig. 13).

Although both models can be equally well fit to the burst interval distributions, we favor the synaptic recovery model. This model is based on measured recovery synaptic rates that are consistent with the interburst intervals, and this model is based on more readily quantifiable parameters that can be subjected to experimental testing.

Implications

An important result of this analysis is that spontaneous transmitter release, which appears to be noise at a single synapse (McCormick 1999; Staley 1999), has a central role in signaling the recovery from depression and driving network output. Thus linking synaptic properties to network behavior is not only important for understanding neural networks but also for understanding the significance of the synaptic properties.

Many neuronal oscillators use membrane conductances for positive and negative feedback. In the bursting CA3 network, positive and negative feedback is provided by depressing recurrent collateral synapses. Thus a network of depressing positive feedback synapses can comprise a distributed synaptic clock (O'Donovan and Rinzel 1997; Tabak et al. 2000; Tsodyks et al. 2000). Such an oscillator contains no pacemaker cells but rather pacemaker synapses that can be tuned by long-term alterations in synaptic strength (Bains et al. 1999; King et al. 1999) (Fig. 10) and synaptic input (Fig. 7B).

One prediction of this analysis is that the smallest increment in burst probability is effected by the gain or loss of a single initiating synapse. As N approaches K (Figs. 8–10), this should be reflected in quantized values of the observed means and variances of the burst interval as synaptic strength is varied. For example, when burst probability is already low, further small decreases in synaptic strength produce a complete cessation of bursting instead of a proportional decrease in the burst frequency (Bains et al. 1999).

The distribution of the intervals between the bursts of a periodically discharging neural network provides information about the level of network excitability and the number of initiating positive feedback synapses. This method can be readily applied to less accessible networks. For example, this analysis would allow an estimation of the amount of positive feedback in an epileptic focus (Lytton et al. 1998; Prince 1999) based on the temporal distribution of electroencepholographic interictal discharges, which might help predict the risk of spontaneous seizures.

REFERENCES

ANDREASEN M, LAMBERT JD, AND JENSEN MS. Effects of new non-N-methyl-D-aspartate antagonists on synaptic transmission in the in vitro rat hippocampus. *J Physiol (Lond)* 414: 317–336, 1989.

BAINS JS, LONGACHER JM, AND STALEY KJ. Reciprocal interactions between CA3 network activity and strength of recurrent collateral synapses. *Nat Neurosci* 2: 720–726, 1999.

BETHEA RM, DURAN BS, AND BOULLION TL. *Statistical Methods for Engineers and Scientists*. New York: Marcel Dekker, 1995, chapt. 3.

BUTTS DA, FELLER MB, SHATZ CJ, AND ROKHSAR DS. Retinal waves are governed by collective network properties. *J Neurosci* 19: 3580–3593, 1999.

CHAMBERLIN NL, TRAUB RD, AND DINGLEDINE R. Role of EPSPs in initiation of spontaneous synchornized burst firing in rat hippocampal neurons bathed in high potassium. *J Neurophysiol* 64: 1000–1008, 1990.

CHURCHLAND PS AND SEJNOWSKI TJ. *The Computational Brain*. Cambridge, MA: MIT Press, 1992, p. 239–306.

COHEN I AND MILES R. Contributions of intrinsic and synaptic activities to the generation of neuronal discharges in in vitro hippocampus. *J Physiol (Lond)* 524: 485–502, 2000.

COLBERT CM, MAGEE JC, HOFFMAN DA, AND JOHNSTON D. Slow recovery from inactivation of Na^+ channels underlies the activity-dependent attenuation of dendritic action potentials in hippocampal CA1 pyramidal neurons. *J Neurosci* 17: 6512–6521, 1997.

CUMMINGS JA, MULKEY RM, NICOLL RA, AND MALENKA RC. Ca^{2+} signalling requirements for long-term depression in the hippocampus. *Neuron* 16: 825–833, 1996.

DEBANNE D, GUÉRINEAU NC, GÄHWILER BH, AND THOMPSON SM. Paired-pulse facilitation and depression at unitary synapses in the rat hippocampus: quantal fluctuation affects subsequent release. *J Physiol (Lond)* 491: 163–173, 1996.

DITTMAN JS, KREITZER AC, AND REGEHR WG. Interplay between facilitation, depression, and residual calcium at three presynaptic terminals. *J Neurosci* 20: 1374–1385, 2000.

DOBRUNZ LE AND STEVENS CF. Heterogeneity of release probability, facilitation, and depletion at central synapses. *Neuron* 18: 995–1008, 1997.

FATT P AND KATZ B. Spontaneous subthreshold activity at motor nerve endings. *J Physiol (Lond)* 117: 109–128, 1952.

FEDIRCHUK B, WENNER P, WHELAN PJ, HO S, TABAK J, AND O'DONOVAN MJ. Spontaneous network activity transiently depresses synaptic transmission in the embryonic chick spinal cord. *J Neurosci* 19: 2102–2112, 1999.

FELLER MB. Spontaneous correlated activity in developing neural circuits. *Neuron* 22: 653–656, 1999.

HAMPSON RE, SIMERAL JD, AND DEADWYLER SA. Distribution of spatial and nonspatial information in dorsal hippocampus. *Nature* 402: 610–614, 1999.

HASTINGS NAJ AND PEACOCK JB. *Statistical Distributions.* New York: Butterworth, 1975, chapt. 2.

JOHNSTON D AND BROWN TH. Control theory applied to neural networks illuminates synaptic basis of interictal epileptiform activity. *Adv Neurol* 44: 263–274, 1986.

KING C, HENZE DA, LEINEKUGEL X, AND BUZSAKI G. Hebbian modification of a hippocampal population pattern in the rat. *J Physiol (Lond)* 521: 159–167, 1999.

LEINEKUGEL X, MEDINA I, KHALILOV I, BEN-ARI Y, AND KHAZIPOV R. Ca^{2+} oscillations mediated by the synergistic excitatory actions of GABA(A) and NMDA receptors in the neonatal hippocampus. *Neuron* 18: 243–255, 1997.

LI XG, SOMOGYI P, YLINEN A, AND BUZSAKI G. The hippocampal CA3 network: an in vivo intracellular labeling study. *J Comp Neurol* 339: 181–208, 1994.

LISMAN J. A mechanism for the Hebb and the anti-Hebb processes underlying learning and memory. *Proc Natl Acad Sci USA* 86: 9574–9578, 1989.

LIU G AND TSIEN RW. Properties of synaptic transmission at single hippocampal synaptic boutons. *Nature* 375: 404–408, 1995.

LIU Q, COULOMBE M, DUMM J, SHAFFER KM, SCHAFFNER AE, BARKER JL, PANCRAZIO JJ, STENGER DA, AND MA W. Synaptic connectivity in hippocampal neuronal networks cultured on micropatterned surfaces. *Brain Res Dev Brain Res* 120: 223–231, 2000.

LYTTON WW, HELLMAN KM, AND SUTULA TP. Computer models of hippocampal circuit changes of the kindling model of epilepsy. *Artif Intell Med* 13: 81–97, 1998.

MAGEE J. Dendritic hyperpolarization-activated currents modify the integrative properties of hippocampal CA1 pyramidal neurons. *J Neurosci* 18: 7613–7624, 1998.

MAGEE J, HOFFMAN D, COLBERT C, AND JOHNSTON D. Electrical and calcium signaling in dendrites of hippocampal pyramidal neurons. *Annu Rev Physiol* 60: 327–346, 1998.

MALENKA RC AND NICOLL RA. Long-term potentiation—a decade of progress? *Science* 285: 1870–1874, 1999.

MARDER E. From biophysics to models of network function. *Annu Rev Neurosci* 21: 25–45, 1998.

MARKRAM H, PIKUS D, GUPTA A, AND TSODYKS M. Potential for multiple mechanisms, phenomena and algorithms for synaptic plasticity at single synapses. *Neuropharmacology* 37: 489–500, 1998.

MARTIN SJ, GRIMWOOD PD, AND MORRIS RGM. Synaptic plasticity and memory: an evaluation of the hypothesis. *Annu Rev Neurosci* 23: 649–711, 2000.

MATVEEV V AND WANG XJ. Implications of all-or-none synaptic transmission and short-term depression beyond vesicle depletion: a computational study. *J Neurosci* 20: 1575–1588, 2000.

MCCORMICK DA. Spontaneous activity: signal or noise? *Science* 285: 541–543, 1999.

MCCORMICK DA AND PAPE HC. Properties of a hyperpolarization-activated cation current and its role in rhythmic oscillation in thalamic relay neurones. *J Physiol (Lond)* 431: 291–318, 1990.

MICKUS T, JUNG HY, AND SPRUSTON N. Properties of slow, cumulative sodium channel inactivation in rat hippocampal CA1 pyramidal neurons. *Biophys J* 76: 846–860, 1999.

MILES R, TOTH K, GULYAS AI, HAJOS N, AND FREUND TF. Differences between somatic and dendritic inhibition in the hippocampus. *Neuron* 16: 815–823, 1996.

MILES R AND WONG RKS. Single neurones can initiate synchronized population discharge in the hippocampus. *Nature* 306: 371–373, 1983.

MILES R AND WONG RK. Excitatory synaptic interactions between CA3 neurones in the guinea-pig hippocampus. *J Physiol* 373: 397–418, 1986.

MILES R, WONG RKS, AND TRAUB RD. Synchronized afterdischarges in the hippocampus: contribution of local synaptic interactions. *Neuroscience* 12: 1179–1189, 1984.

MURTHY VN, SEJNOWSKI TJ, AND STEVENS CF. Heterogeneous release properties of visualized individual hippocampal synapses. *Neuron* 18: 599–612, 1997.

O'DONOVAN MJ AND RINZEL J. Synaptic depression: a dynamic regulator of synaptic communication with varied functional roles. *Trends Neurosci* 20: 431–433, 1997.

OTIS T, ZHANG S, AND TRUSSELL LO. Direct measurement of AMPA receptor desensitization induced by glutamatergic synaptic transmission. *J Neurosci* 16: 7496–7504, 1996.

PRESS WH, TEUKOLSKY SA, VETTERLING WT, AND FLANNERY BP. *Numerical Recipes in Fortran 77.* New York: Cambridge Press, 1997, chapt. 6.

PRANGE O AND MURPHY TH. Correlation of miniature synaptic activity and evoked release probability in cultures of cortical neurons. *J Neurosci* 19: 6427–6438, 1999.

PRINCE DA. Epileptogenic neurons and circuits. *Adv Neurol* 79: 665–684, 1999.

REID CA AND CLEMENTS JD. Postsynaptic expression of long-term potentiation in the rat dentate gyrus demonstrated by variance-mean analysis. *J Physiol (Lond)* 518.1: 121–130, 1999.

ROBINSON JH AND DEADWYLER SA. Kainic acid produces depolarization of CA3 pyramidal cells in the vitro hippocampal slice. *Brain Res* 221: 117–127, 1981.

ROBINSON HP, KAWAHARA M, JIMBO Y, TORIMITSU K, KURODA Y, AND KAWANA A. Periodic synchronized bursting and intracellular calcium transients elicited by low magnesium in cultured cortical neurons. *J Neurophysiol* 70: 1606–1616, 1993.

SCANZIANI M, CAPOGNA M, GÄHWILER BH, AND THOMPSON SM. Presynaptic inhibition of miniature excitatory synaptic currents by baclofen and adenosine in the hippocampus. *Neuron* 9: 9–27, 1992.

SEGAL MM AND FURSHPAN EJ. Epileptiform activity in microcultures containing small numbers of hippocampal neurons. *J Neurophysiol* 64: 1390–1399, 1990.

SELIG DK, NICOLL RA, AND MALENKA RC. Hippocampal long-term potentiation preserves the fidelity of postsynaptic responses to presynaptic bursts. *J Neurosci* 19: 1236–1246, 1999.

STALEY KJ. Quantal GABA release: noise or not? *Nat Neurosci* 2: 494–495, 1999.

STALEY KJ, LONGACHER M, BAINS JS, AND YEE A. Presynaptic modulation of CA3 network activity. *Nat Neurosci* 1: 201–209, 1998.

STALEY KJ AND MODY I. Shunting of excitatory input to dentate gyrus granule cells by a depolarizing GABAA receptor-mediated postsynaptic conductance. *J Neurophysiol* 68: 197–212, 1992.

STASHEFF SF, ANDERSON WW, CLARK S, AND WILSON WA. NMDA antagonists differentiate epileptogenesis from seizure expression in an in vitro model. *Science* 245: 648–651, 1989.

STEVENS CF AND WESSELING JF. Activity-dependent modulation of the rate at which synaptic vesicles become available to undergo exocytosis. *Neuron* 21: 415–424, 1998.

STEVENS CF AND WESSELING JF. Identification of a novel process limiting the rate of synaptic vesicle cycling at hippocampal synapses. *Neuron* 24: 1017–1028, 1999.

SWARTZWELDER HS, LEWIS DV, ANDERSON WW, AND WILSON WA. Seizure-like events in brain slices: suppression by interictal activity. *Brain Res* 410: 362–366, 1987.

TABAK J, SENN W, O'DONOVAN MJ, AND RINZEL J. Modeling of spontaneous activity in developing spinal cord using activity-dependent depression in an excitatory network. *J Neurosci* 20: 3041–3056, 2000.

TRAUB RD AND DINGLEDINE R. Model of synchronized epileptiform bursts induced by high potassium in CA3 region of rat hippocampal slice. Role of spontaneous EPSPs in initiation. *J Neurophysiol* 64: 1009–1018, 1990.

TRAUB RD AND MILES R. *Neuronal Networks of the Hippocampus.* Cambridge, UK: Cambridge Univ. Press, 1991, chapt. 6.

TRAUB RD AND WONG RKS. Cellular mechanisms of neuronal synchronization in epilepsy. *Science* 216: 745–747, 1982.

TSODYKS M, UZIEL A, AND MARKRAM H. Synchrony generation in recurrent networks with frequency dependent synapses. *J Neurosci* 20 (RC 50): 1–5, 2000.

WU LG AND BORST JG. The reduced release probability of releasable vesicles during recovery from short-term synaptic depression. *Neuron* 23: 821–832, 1999.

XIONG ZQ AND STRINGER JL. Cesium induces spontaneous epileptiform activity without changing extracellular potassium regulation in rat hippocampus. *J Neurophysiol* 82: 3339–3346, 1999.